Journal of Power Sources 195 (2010) 142–145

Contents lists available at ScienceDirect

Journal of Power Sources

journal homepage: www.elsevier.com/locate/jpowsour

Short communication

A novel bifunctional electrocatalyst for unitized regenerative fuel cell

Yining Zhang[a,b], Huamin Zhang[a,*], Yuanwei Ma[a,b], Jinbin Cheng[a,b], Hexiang Zhong[a], Shidong Song[a,c], Haipeng Ma[a]

[a] Lab of PEMFC Key Materials and Technologies, Dalian Institute of Chemical Physics, Chinese Academy of Sciences, Dalian 116023, China
[b] Graduate School of the Chinese Academy of Sciences, Beijing 100039, China
[c] School of Chemistry, University of St. Andrews, North Haugh, St. Andrews, Fife KY16 9ST, UK

ARTICLE INFO

Article history:
Received 12 June 2009
Received in revised form 8 July 2009
Accepted 9 July 2009
Available online 18 July 2009

Keywords:
Unitized regenerative fuel cell
Platinum supported on iridium oxide
Bifunctional oxygen electrode
Electrocatalyst
Fuel cell
Water electrolysis

ABSTRACT

5 wt.% of platinum (Pt) nanoparticles are highly dispersed on the surface of IrO_2 by chemical reduction, and the catalyst is mixed with Pt black to be used as a novel bifunctional oxygen electrocatalyst for the unitized regenerative fuel cell (URFC). The novel cell has been evaluated in the hydrogen and oxygen fuel cell and water electrolysis modes, and compared to a similar cell with an oxygen electrode using conventional mixed Pt black and IrO_2 catalyst. With the novel oxygen electrode catalyst, the highest fuel cell power density is 1160 mW cm^{-2} at 2600 mA cm^{-2}; the overall performance is close to that with the commercial Pt supported on carbon catalyst and about 1.8 times higher than that with the conventional mixed Pt black and IrO_2 catalyst. Additionally, the cell performance for water electrolysis is also slightly improved, which is probably the result of lower interparticle catalyst resistance with 5 wt.% Pt on IrO_2 compared to no Pt on IrO_2.

1. Introduction

Unitized regenerative fuel cells (URFCs) are electrochemical cells working both as fuel cells and water electrolyzers. In water electrolysis mode, the water is electrolyzed to hydrogen and oxygen which are recombined to produce electricity in the subsequent fuel cell mode. With the advantages of being free of self-discharge and theoretically higher energy densities, URFCs are especially considered as the promising energy storage systems for space applications [1].

The key technology in the development of URFC is the fabrication of active electrocatalyst for oxygen redox reaction at the oxygen electrode. Carbon black, the catalyst support widely used in fuel cells, is not suitable for URFC due to its corrosion at high voltage especially in water electrolysis mode [2]. Therefore, the bifunctional oxygen electrode electrocatalysts of URFC are generally unsupported, causing their low activity and high loading. Normally, the conventional Pt catalyst for oxygen reduction reaction (ORR) is mixed with oxide catalysts of Ir or Ru for oxygen evolution reaction (OER) to be used as the bifunctional electrocatalyst [3,4]. As shown in Fig. 1a, the unsupported particles of Pt or oxide can easily aggregate to form large agglomerations which are hardly well dispersed in the solvent, resulting in poor interdispersion of the two kinds of electrocatalysts and low bifunctional performance. To resolve the problem, some researchers [5,6] prepared supported bifunctional electrocatalysts through depositing the two kinds of catalysts on each other respectively using Pt or oxide as support. Unlike carbon black, neither Pt nor IrO_2 is excellent support for obtaining highly dispersed particles with high loading, thus significant improvements of the electrocatalyst activity for both ORR and OER could not be achieved by the methods mentioned above. Moreover, the activity of the Pt supported on IrO_2 (40 wt.% Pt) bifunctional catalyst for ORR was lower than that of the mixed Pt black and IrO_2 catalyst [6].

In this paper, the Pt supported on IrO_2 (5 wt.% Pt) catalyst has been prepared by chemical reduction of H_2PtCl_6 on the surface of IrO_2 and mixed with Pt black to be used as the bifunctional oxygen electrode electrocatalyst. The novel electrocatalyst composition, as shown in Fig. 1b, provides three advantages as follows. Firstly, with lower loading of Pt in the preparation process of Pt/IrO_2, high dispersion as well as good size control of Pt NPs on the surface of IrO_2 aggregations can be easily obtained, which is quite beneficial to improving the catalyst activity. Secondly, the supported Pt NPs can also contribute to ORR leading to a better use of the space occupied by IrO_2. Thirdly, the IrO_2 aggregations are surrounded by the supported Pt NPs, maintaining the electron pathways as in the IrO_2/Pt electrocatalyst reported by Ioroi et al. [5].

Using the novel electrocatalyst, a single cell has been fabricated and evaluated to make a comparison to the traditional cell.

* Corresponding author. Tel.: +86 411 84379072; fax: +86 411 84665057.
E-mail address: zhanghm@dicp.ac.cn (H. Zhang).

0378-7753/$ – see front matter © 2009 Elsevier B.V. All rights reserved.
doi:10.1016/j.jpowsour.2009.07.018

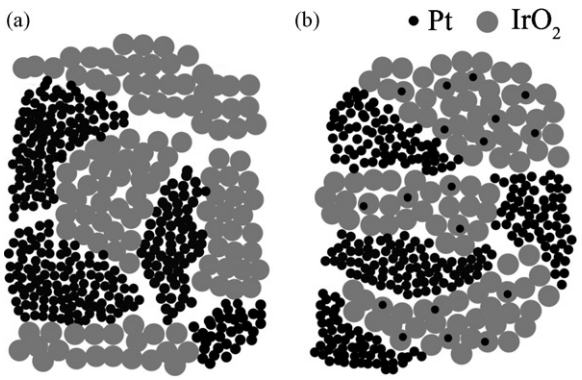

Fig. 1. Schematic diagrams: (a) mixed Pt and IrO_2 and (b) mixed Pt and Pt/IrO_2.

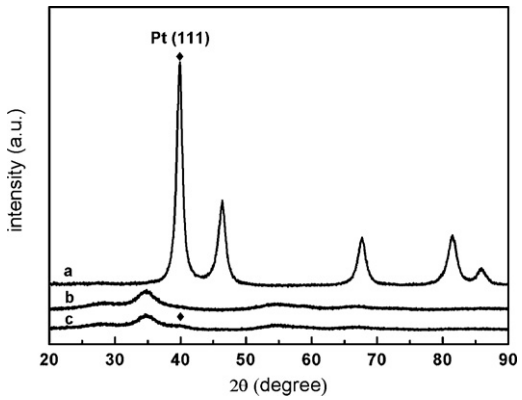

Fig. 2. XRD patterns of the samples: (a) Pt black, (b) IrO_2 and (c) Pt/IrO_2.

2. Experimental

2.1. Preparation of the Pt/IrO_2

Pt/IrO_2 (5 wt.% Pt) electrocatalyst was prepared by chemical reduction of H_2PtCl_6 on IrO_2 aggregations. Formaldehyde was used as the reducing agent. IrO_2, which was used as support as well as electrocatalyst for OER, was prepared using Adams method [7]. In a typical preparation process, 190 mg IrO_2 (847.4 μmol) was suspended in 100 ml deionized water and ultrasonicated for 30 min, before 1 ml H_2PtCl_6 aqueous solution containing 10 mg Pt (51.3 μmol) was added under continuously magnetic stirring. Then the pH of the solution was adjusted to 9.0 by dropwise addition of 0.5 M Na_2CO_3 aqueous solution. The mixture was held at room temperature for 10 h under magnetic stirring and nitrogen bubbling. Subsequently, 1 ml formaldehyde aqueous solution (40 wt.% formaldehyde) was added into the mixture in an oil bath at 85 °C, then the resulting reaction mixture was aged for 60 min, followed by being cooled to room temperature, centrifuged rinsed for several times with deionized water and dried in a vacuum oven.

2.2. Characterizations of the electrocatalysts

XRD analyses were performed using a Philips CM-1 Power diffractometer with a Cu Kα radiation resource to determine the crystalline structure of all the samples. The morphology of the catalysts was characterized with JEOL JEM-2000EX at 120 kV for low-resolution TEM test and TECNAI F30 at 300 kV for high-resolution TEM test. In addition, ICP test was carried out using PerkinElmer 2000 DV to determine the Pt content of the Pt/IrO_2 catalyst.

2.3. Fabrications and evaluations of single cells

The mixture of catalyst and Nafion in isopropanol (10 mg catalyst ml isopropanol^{-1}) was sprayed onto the gas diffusion layer (GDL) to form the gas diffusion electrode (GDE). The Nafion 212 membrane was sandwiched between the hydrogen GDE and the oxygen GDE, followed by a hot treatment at 160 °C under 1 MPa for 1 min to obtain MEA. Pt/C (28.4 wt.%, T.K.K. Corp.) was used for hydrogen electrode with a Pt loading of 0.2 mg cm^{-2}, and the mixed Pt black (T.K.K. Corp.) and Pt/IrO_2 (weight ratio, $Pt:Pt/IrO_2 = 100:100$) for oxygen electrode with a total catalyst loading of 1 mg cm^{-2}. The Nafion® content was 25% for hydrogen electrode and 20% for oxygen electrode, and the single cell was named as URFC1. For comparison, a single cell named as URFC2 with the mixed Pt black and IrO_2 (weight ratio, Pt: $IrO_2 = 105:95$) with the same loading, as well as a fuel cell using Pt/C (47.6 wt.%, T.K.K. Corp.) as oxygen electrode electrocatalyst with a Pt loading of 0.5 mg cm^{-2} was prepared.

The cell performance with an active area of 5 cm^2 was evaluated as described in a previous paper [4]. During fuel cell mode, the URFC was operated at 80 °C with H_2/O_2 at pressure of 0.2 MPa. The reactant gases, hydrogen and oxygen, were externally humidified before entering the test cell by bubbling them through the water at 90 °C and 85 °C respectively. During water electrolysis mode, deionized water was pumped into the oxygen electrode from water reservoir kept at 80 °C at atmospheric pressure. The polarization

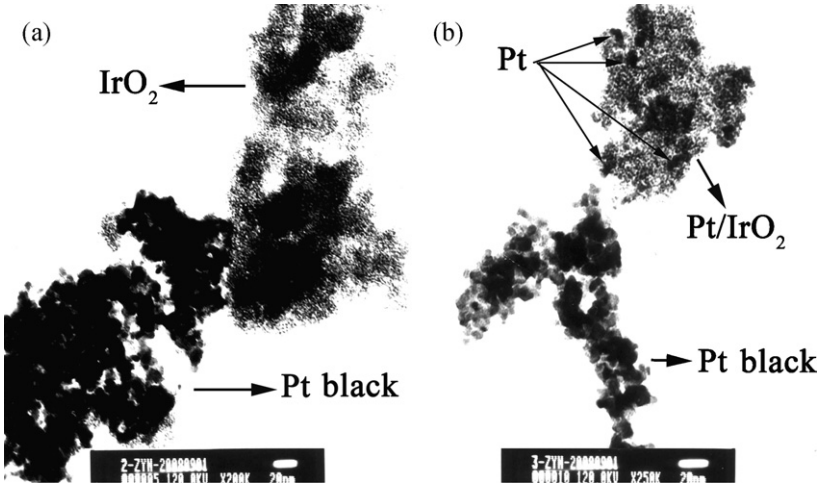

Fig. 3. Low-resolution TEM images of the samples: (a) mixed Pt black and IrO_2 and (b) mixed Pt black and Pt/IrO_2.

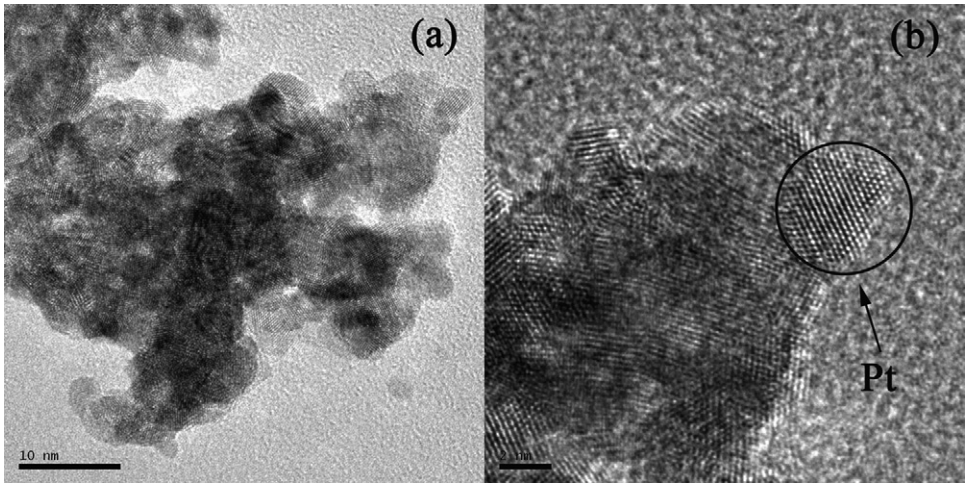

Fig. 4. High-resolution TEM images of Pt/IrO_2.

curves of the URFCs were galvanostatically measured at constant current.

Electrochemical impedance spectroscopy (EIS) of the URFCs in fuel cell mode was recorded using a KFM2030 impedance meter (Kikusui, Japan) with frequency from 10 kHz to 100 mHz and the superposed current was 165 mA. EIS in water electrolysis mode was recorded using PARSTAT 2273 (AMETEK, USA) at 1.45 V with frequency from 100 kHz to 10 mHz and the amplitude of the sinusoidal potential perturbation was 10 mV. Oxygen electrode was used as working electrode, and hydrogen electrode was used as both reference and counter electrodes.

3. Results and discussion

Fig. 2 shows the XRD patterns of all the samples. The diffraction peaks of Pt black (T.K.K. Corp.) corresponding to different planes can be observed from the pattern obviously. The XRD patterns of IrO_2 and Pt/IrO_2 are almost the same except that Pt/IrO_2 has a minor diffraction peak at 2θ value of 39.9° corresponding to the Pt (1 1 1) plane, demonstrating the presence of Pt in Pt/IrO_2. Nevertheless, the other diffraction peaks of Pt cannot be found from the XRD pattern of Pt/IrO_2, ascribed to the low loading of Pt and the relatively amorphous nature of IrO_2. In addition, ICP result shows that the Pt content in Pt/IrO_2 is 4.5%, nearly equal to the designed value.

TEM images of all the samples are presented in Figs. 3 and 4. As shown in Fig. 3a, the mixed Pt black and IrO_2 aggregations are poorly interdispersed. In Fig. 3b, the morphology of the catalyst looks similar to that shown in Fig. 3a except that on the surface of IrO_2 aggregations presenting some highly dispersed Pt NPs distinguished by the difference in the contrast of the two kinds of catalysts. The high-resolution TEM image of Pt/IrO_2 is shown in Fig. 4. In the edge region of the catalyst aggregations, a single Pt NP with a diameter of about 5 nm is marked by the interplanar distance of Pt (1 1 1) (d_{111} = 0.2265 nm), also indicating the high dispersion of Pt NPs.

Fig. 5a shows EIS of URFC1 and URFC2 in fuel cell mode at 500 mA cm^{-2}. The high frequency intercept with real axes is the internal resistance (R_i) of the cells, including the electronic resistance due to the GDLs and the flow-fields, the ionic resistance of the membrane, and a function of the electronic and ionic resistance of the catalyst layer (CL). The arc diameter is a measure of the polarization resistance (R_p) of ORR mainly corresponding to the three-phase boundary of electrocatalyst, electrolyte and gas [8–10]. Compared to URFC2, both R_i and R_p of URFC1 are lower at 500 mA cm^{-2}, and the R_p is decreased by about one half. As the structure components of the two cells are approximately identical except for CLs, the differences in R_i and R_p should be caused by the catalyst composition. As indicated by the TEM images, the Pt NPs supported on IrO_2 aggregations provide better electronic pathways for their higher electronic conductivity compared with IrO_2 in CL, as revealed by the decrease in the R_i. Likewise, the three-phase boundary where Pt, Nafion and oxygen meet is also enlarged attributed to the better use of the space occupied by IrO_2 through the supported Pt NPs, leading to the decrease in R_p.

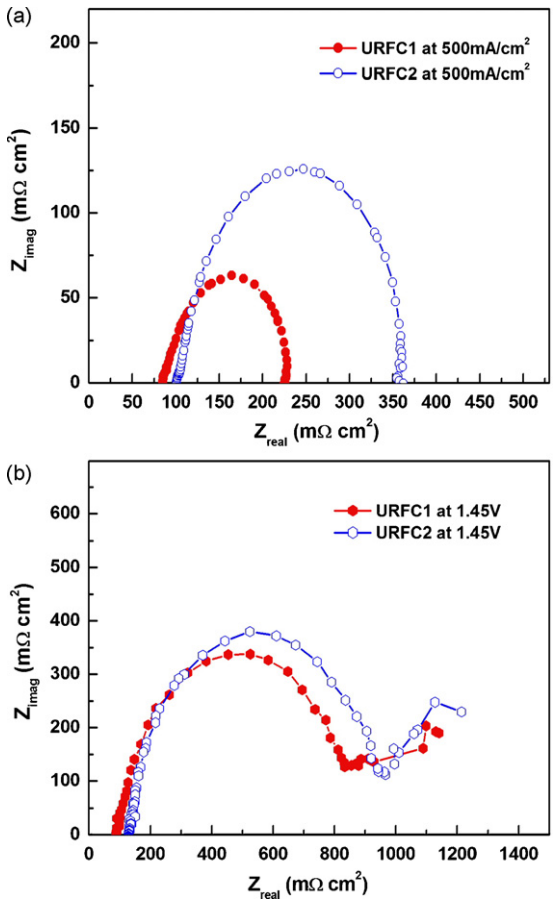

Fig. 5. EIS of the URFCs: (a) in fuel cell mode and (b) in water electrolysis mode.

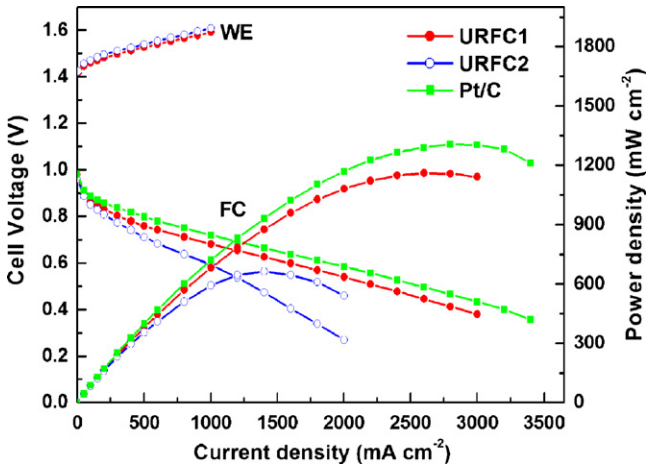

Fig. 6. Cell performance of URFCs and a single fuel cell.

Fig. 5b shows the EIS of the two cells in water electrolysis mode at 1.45 V. Similar to that in fuel cell mode, the R_i of URFC1 is lower due to the same reason mentioned above. In contrast, the difference in the arc diameters of the two cells is not as large as that in fuel cell mode, ascribed to the same morphology and dispersion of IrO_2 in the CL. Because of the better electronic pathways maintained by the supported Pt NPs around the IrO_2 aggregations and higher OER activity of Pt/IrO_2 attributed to the interaction between Pt and IrO_2 as analyzed by Yao et al. [6], the arc diameter of URFC1 is relatively smaller than that of URFC2.

As shown in Fig. 6, URFC1 obtains a better cell performance than URFC2, especially in fuel cell mode. The gap in cell voltage is 91 mV at 1000 mA cm^{-2}, and becomes even larger as the current density increases. The highest power density of URFC1 is 1160 mW cm^{-2} at 2600 mA cm^{-2}, which is about 1.8 times higher than that of URFC2. In addition, the cell performance of URFC1 in fuel cell mode is close to that of a fuel cell using commercial Pt/C as oxygen electrode electrocatalyst, as shown in Fig. 6. The cell performance in water electrolysis mode is also improved, and the cell voltage is decreased by 16 mV at 1000 mA cm^{-2}.

4. Conclusions

Pt/IrO_2 (5 wt.% Pt) has been prepared by chemical reduction of Pt on the surface of IrO_2, and high dispersion of Pt NPs is obtained ascribed to the lower loading. With the mixture of Pt/IrO_2 and Pt black as bifunctional oxygen electrocatalyst, the internal resistance of the cell is decreased, and the space occupied by the IrO_2 is better used by the supported Pt NPs in fuel cell mode compared to the traditional electrocatalyst. The cell performance in fuel cell mode is dramatically improved, quite close to that a single fuel cell using commercial Pt/C as oxygen electrode electrocatalyst, and the cell performance in water electrolysis mode is also improved.

Acknowledgements

This work is supported by the National High Technology Research and Development Program of China (863 Program), No. 2007AA05Z129 and No. 2007AA11A106. The authors thank Zhen Yin for the help on the HRTEM characterization.

References

[1] W. Smith, J. Power Sources 86 (2000) 74.
[2] K.H. Kangasniemi, D.A. Condit, T.D. Jarvi, J. Electrochem. Soc. 151 (2004) E125.
[3] T. Ioroi, N. Kitazawa, K. Yasuda, Y. Yamamoto, J. Electrochem. Soc. 147 (2000) 2018.
[4] S. Song, H. Zhang, X. Ma, Z.-G. Shao, Y. Zhang, B. Yi, Electrochem. Commun. 8 (2006) 399.
[5] T. Ioroi, N. Kitazawa, K. Yasuda, Y. Yamamoto, H. Takenaka, J. Appl. Electrochem. 31 (2001) 1179.
[6] W. Yao, J. Yang, J. Wang, Y. Nuli, Electrochem. Commun. 9 (2007) 1029.
[7] R. Adams, R.L. Shriner, J. Am. Chem. Soc. 45 (1923) 2171.
[8] P.M. Gomadam, J.W. Weidner, Int. J. Energy Res. 29 (2005) 1133.
[9] X. Yuan, H. Wang, J.C. Sun, J. Zhang, Int. J. Hydrogen Energy 32 (2007) 4365.
[10] J. Wu, X.Z. Yuan, H. Wang, M. Blanco, J.J. Martina, J. Zhang, Int. J. Hydrogen Energy 33 (2008) 1735.